metals

MDPI

Article

Formation Process of Long-Period Stacking-Ordered Structures in $Mg_{97}Zn_1Y_2$ Alloy Comprising HCP and Cubic Phases Fabricated by High-Pressure High-Temperature Annealing

Atsuki Yokota [1], Masafumi Matsushita [1,2,*], Naruhito Geshi [1], Daiki Yamasaki [1], Toru Shinmei [2], Michiaki Yamasaki [3] and Yoshihito Kawamura [3]

[1] Department of Mechanical Engineering, Ehime University, 3-Bunkyocho, Matsuyama 790-0826, Japan; yokota.atsuki.lt@ehime-u.ac.jp (A.Y.); g840024m@mails.cc.ehime-u.ac.jp (N.G.); h840048b@mails.cc.ehime-u.ac.jp (D.Y.)
[2] Geodynamics Research Center, Ehime University, 2-Bunkyocho, Matsuyama 790-0826, Japan; shinmei@sci.ehime-u.ac.jp
[3] Magnesium Research Center, Kumamoto University, Kumamoto 860-8555, Japan; yamasaki@gpo.kumamoto-u.ac.jp (M.Y.); rivervil@gpo.kumamoto-u.ac.jp (Y.K.)
* Correspondence: matsushita.masafumi.me@ehime-u.ac.jp; Tel.: +81-899-279-902

Abstract: As-cast $Mg_{97}Zn_1Y_2$ alloy consists of α-Mg matrix and 18R-type long-period stacking-ordered (LPSO) structures. We observed that the alloy undergoes a phase transformation to $D0_3$ superlattices and α-Mg matrix due to high-pressure high-temperature (HPHT) annealing at 3 GPa and above 773 K. Further, the alloy recovered after HPHT annealing, consisting of the α-Mg matrix and $D0_3$ superlattices, transformed into 18R-type LPSO structures during further annealing at ambient pressure. An fcc structure with a lattice parameter of 1.42 nm, which was twice that of $D0_3$, emerged in both the collapse process of the 18R-type LPSO structure under high-pressure, and the formation process of the 18R-type LPSO structure at ambient pressure. This fcc phase was an intermediate structure between 18R-type LPSO and $D0_3$. From the electron diffraction results, it is considered that 18R-type LPSO is continuously present with 2H including stacking faults, which almost corresponded with previous studies.

Keywords: Mg–Zn–Y ternary alloys; long-period stacking-ordered structure; high-pressure treatment; X-ray diffraction; transmission electron microscopy

Citation: Yokota, A.; Matsushita, M.; Geshi, N.; Yamasaki, D.; Shinmei, T.; Yamasaki, M.; Kawamura, Y. Formation Process of Long-Period Stacking-Ordered Structures in $Mg_{97}Zn_1Y_2$ Alloy Comprising HCP and Cubic Phases Fabricated by High-Pressure High-Temperature Annealing. *Metals* **2021**, *11*, 1031. https://doi.org/10.3390/met11071031

Academic Editor: Anders E. W. Jarfors

Received: 30 April 2021
Accepted: 23 June 2021
Published: 26 June 2021

1. Introduction

Long-period stacking-ordered (LPSO) structures in magnesium (Mg) ternary alloys consisting of rare earth (RE) and another metal (M) have piqued interest as a potential strengthening approach [1–3]. The strength of Mg alloys consisting of α-Mg matrix and LPSO structures is greatly increased when the LPSO structure is kinked by plastic deformation. The LPSO structures in Mg–M–RE alloys have been studied using high-angle annular dark-field scanning transmission electron microscopy (HAADEF-STEM), and then the crystal structures of some kinds of LPSO were determined [4–6]. In these LPSO structures are characterized stacking faults (SFs) inserted periodically in ABAB stacking, and $L1_2$-type clusters of M_6RE_8 in the SFs [5,6]. Further, an interstitial Mg atom exists in a body center of the $L1_2$-type cluster, which makes the LPSO energetically stable [7].

The formation process of LPSO structures is interesting from the viewpoint of the physics of metals and for development of materials strengthened by kinked bands. Therefore, LPSO structure formation processes have been investigated on both experimental and computational methods [8–17].

Our group studied the pressure-induced phase transition of the 18R-type LPSO in Mg–Zn–Y ternary alloys. $Mg_{85}Zn_6Y_9$ possessed 18R-type LPSO monophase at ambient pressure and is in contact with a liquid phase at high temperatures [18]. However, by in

situ X-ray diffraction (XRD) at 3 GPa, 18R-type LPSO structures in $Mg_{85}Zn_6Y_9$ transform into the α-Mg and $D0_3$ phases with an increase in temperature [19]. The alloy recovered after being subjected to 7 GPa at 973 K revealed a fine dual-phase structure composed of $D0_3$ and α-Mg ($D0_3$/α-Mg) [20]. The $D0_3$/hcp structure in $Mg_{85}Zn_6Y_9$ transformed into the 18R-type LPSO when heated at ambient pressure [13]. In situ XRD revealed that the lattice volume of α-Mg(2H) initially increased with an increase in the temperature due to the intrusion of Y emitted from $D0_3$ into the 2H lattice. After that, the 2H structure collapsed due to the formation of random SFs, causing the formation of 18R-type LPSO structures. Further, first-principles calculation explained that the formation process of 18R-type LPSO structure resulted from two factors: the thermodynamic instability of the 2H stacking and the segregation of Y and Zn into the SF layer [9,13].

In this paper, first, we reported the effect of pressure on the $Mg_{97}Zn_1Y_2$ alloy with the α-Mg matrix and an 18R-type LPSO structure. The 18R-type LPSO was decomposed to $D0_3$/hcp by high-pressure high-temperature (HPHT) treatments. Then, we reported the process of the 18R-type LPSO phase formation from $D0_3$/hcp fabricated by the HPHT-treatment.

2. Materials and Methods

$Mg_{97}Zn_1Y_2$ alloy ingot was made by casting, and an inductively coupled plasma optical emission spectrometer (Shimazu ICPS-8100, Kyoto, Japan) was used to ascertain its chemical composition. The alloy was cut into a columnar shape of 2 mm in diameter and 5 mm in length for high-pressure experiments. The high-pressure condition was generated by the multi-anvil high-pressure apparatus (CTF Co., Tokyo, Japan). MgO was used as the octahedron high-pressure cells and sample capsules, whereas graphite and tungsten carbide was used as a heater and secondary anvil, respectively. The annealing of the alloys after HPHT treatment was realized in an evacuated silica tube and subsequently quenched in water. XRD was conducted using Cu-Kα radiation (Rigaku., RAPIDII-V/DW, Japan). The X-ray incident angle was fixed at 2°, and the diffracted pattern was detected using an imaging plate. The microstructures were observed using a backscattered electron (BE) image of scanning electron microscopy (SEM: JEOL, JSM-7000F, Japan). Electron diffraction (ED) was observed via transmission electron microscopy (TEM: JOEL, JEM-2010, Japan). Sample preparation for TEM was realized by a focused ion beam (FIB; FEI, SCIOS, USA). XRD and ED results were analyzed using simulation software CrystalDiffract6 (CrystalMaker Software Limited., Begbroke, UK) and ReciPro ver.4 (open source software, Tokyo, Japan), respectively.

3. Results and Discussion

Figure 1 shows the XRD patterns of the $Mg_{97}Zn_1Y_2$ cast alloy and the alloy recovered after being annealed at 3 GPa for 2 h at various temperatures. The XRD peaks of the cast alloy may be attributed to the α-Mg, 18R-type LPSO, and some impurities (Y, and Y_2O_3). For the alloy annealed at 3 GPa and 773 K, however, certain peaks (designated as E_1, E_2, and E_3) were confirmed. The peaks almost corresponded to that of the E phase with a large cubic lattice, reported previously in the $Mg_{85}Zn_6Y_9$ alloy [13]. Only the peaks from the hcp and high-pressure phase ($D0_3$) were obtained by raising the annealing temperature beyond 823 K, whereas peaks from the 18R-type LPSO and E phase disappeared completely. The crystal information of $D0_3$ estimated from XRD intensity, which is similar to that the HPHT phase of $Mg_{75.5}Zn_{9.5}Y_{13.8}$ [21]. These results indicated that the transformation from 18R-type LPSO/α-Mg to $D0_3$/α-Mg occurs at 3 GPa with an increase in temperature, and the phase suggested by E_1, E_2, and E_3 peaks existed as an intermediate phase during the phase transformation.

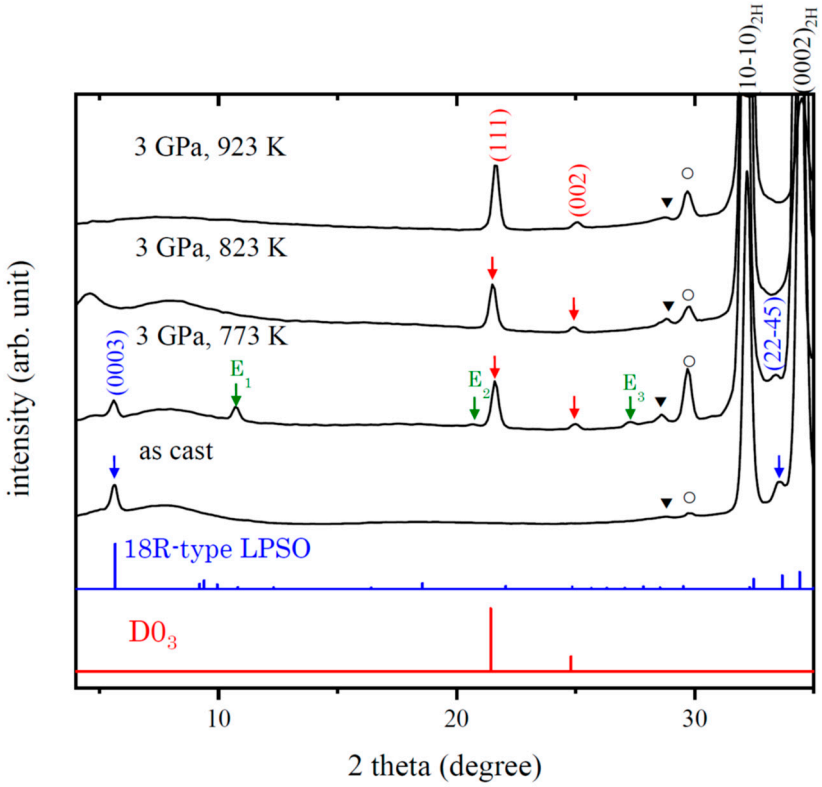

Figure 1. X-ray diffraction patterns of $Mg_{97}Zn_1Y_2$ cast alloy and the alloy recovered after being annealed at 3 GPa for 2 h at various temperatures. The blue and red lines show the estimated peak position and intensity from the 18R-type LPSO [5] and $D0_3$ superlattice listed in Table 1, respectively. The index and arrows in blue and red indicate coinciding peaks to 18R-type LPSO and $D0_3$, respectively. The peaks from Y_2O_3 and Y are indicated by a circle (○) and triangle (▼), respectively.

Table 1. Crystal information of high-pressure phase ($D0_3$) estimated by XRD. Chemical composition: $Mg_{63}Zn_{16.5}Y_{20.5}$, Space group: $Fm\bar{3}m$, Lattice constant: 0.71 nm.

Element	X	Y	Z	Site Occupancy
Mg	0.50	0.50	0.50	1
Mg	0.25	0.25	0.25	0.67
Mg	0.00	0.00	0.00	0.18
Y	0.00	0.00	0.00	0.82
Zn	0.25	0.25	0.25	0.33

Figure 2a,b shows the compositional images in the BE mode of SEM for the $Mg_{97}Zn_1Y_2$ cast alloy and the alloy recovered after being annealed at 3 GPa and 823 K, respectively. Figure 2a shows the bright 18R-type LPSO phase and the boundary of the dark α-Mg matrix. The 18R-type LPSO surrounds α-Mg, which is characteristic of LPSO microstructures and agrees with previous reports [22]. Figure 2b shows that the thin $D0_3$ phase exists around the matrix. The volume fraction of the $D0_3$ phase is smaller than that of the 18R-type LPSO phase shown in Figure 2a. This result is plausible to insinuate that the atomic density of the $D0_3$ structure is higher than that of the 18R-type LPSO structure. In addition, the concentration of Y and Zn are higher than those of the 18R-type LPSO as shown in Table 1.

Subsequently, the process of the 18R-type LPSO structure formation from $D0_3$/α-Mg at ambient pressure was investigated. The $Mg_{97}Zn_1Y_2$ alloy recovered after being annealed at 3 GPa and 823 K for 2 h was made the starting material. XRD, SEM, and TEM were used to analyze the crystal structure and microstructural variations of the alloy caused by further annealing for 10 min at ambient pressure. The XRD patterns of the alloy annealed

at various temperatures are shown in Figure 3. In the XRD pattern of the alloy annealed at 623 K, $(0003)_{18R}$, E_1, E_2, and E_3 peaks emerged. Further, at 643 K, a new peak indicated as ◇ emerged. Peaks labeled E_1, E_2, and E_3 disappeared in the XRD pattern of the alloy annealed at 673 K. Finally, the peaks from $D0_3$ disappeared, and the XRD patterns of the alloy annealed at 723 K completely corresponded to the as-cast $Mg_{97}Zn_1Y_2$ alloy.

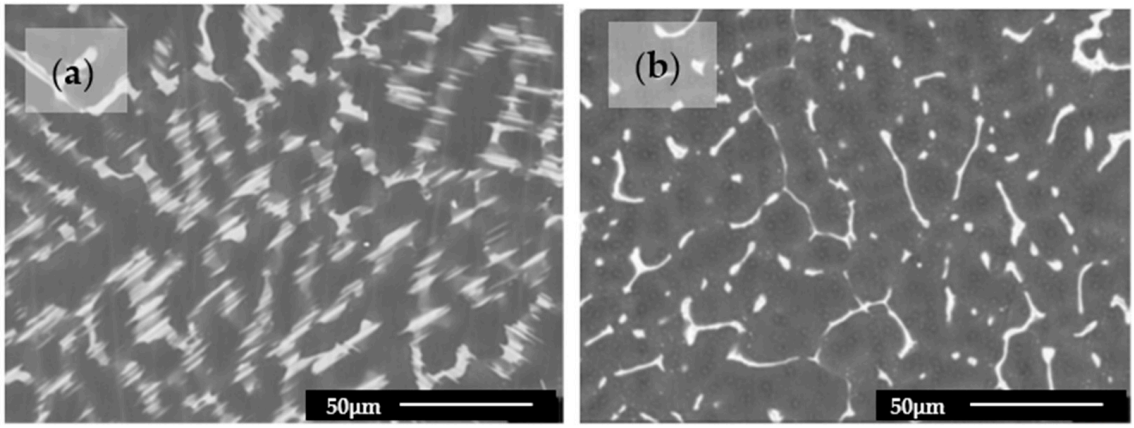

Figure 2. (**a**) Backscattered electron mode of scanning electron microscopy of the $Mg_{97}Zn_1Y_2$ cast alloy and (**b**) the alloy recovered after being annealed at 3 GPa and 823 K.

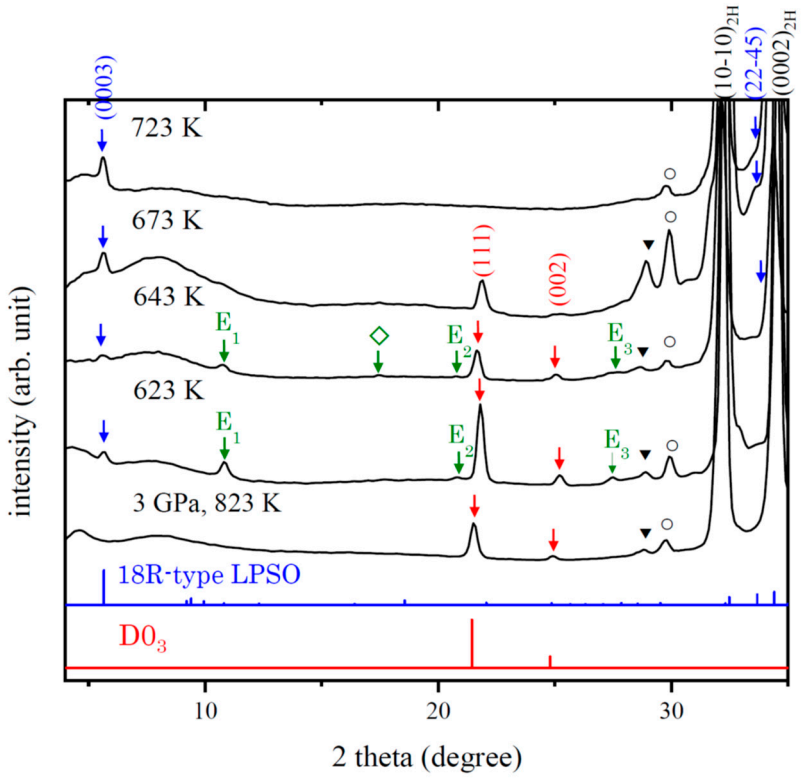

Figure 3. X-ray diffraction patterns of the $Mg_{97}Zn_1Y_2$ alloy, which had been annealed at 3 GPa and 823 K for 2 h, and subsequently annealed for 10 min at various temperatures in ambient pressure. The blue and red lines show the estimated peak position and intensity from the 18R-type LPSO in Reference [5] and $D0_3$ in Table 1, respectively. The index and arrows in blue and red indicate coinciding peaks to 18R-type LPSO and $D0_3$, respectively. The peaks from Y_2O_3 and Y are indicated by a circle (○) and triangle (▼), respectively.

Figure 4 shows the compositional images in the BE mode of SEM for alloys corresponding to the XRD patterns in Figure 3. Fine-threads bright phase precipitates were observed in the alloy annealed at 623 K in Figure 4a, which is identical to that in Figure 2b. XRD peaks corresponding to 18R-type LPSO structure were confirmed in the alloy, however, the characteristic microstructure of LPSO shown in Figure 2a, was not observed. The bright phase gets thicker in the alloy annealed at 643 K, as shown in Figure 4b. The microstructure in Figure 4c approaches that of the LPSO phase in Figure 2a when the temperature rises.

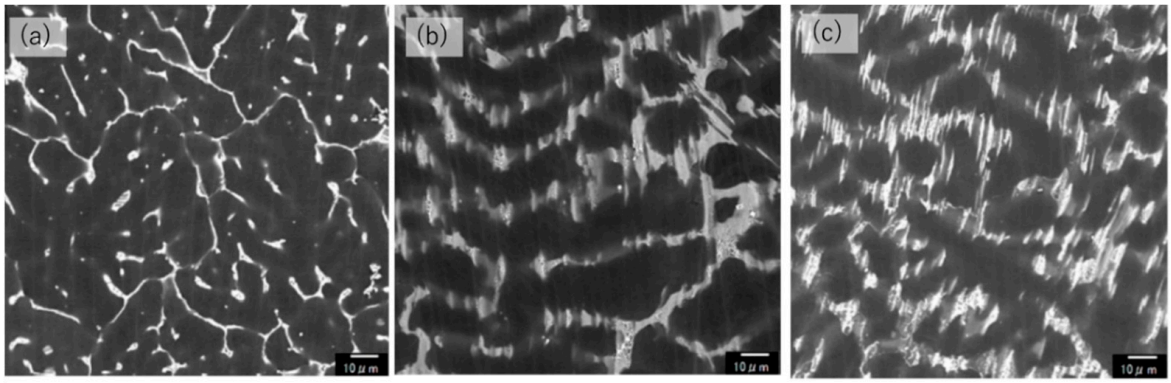

Figure 4. (**a**) Backscattered electron mode of scanning electron microscopy of the $Mg_{97}Zn_1Y_2$ alloy, which had been recovered after being annealed at 3 GPa and 823 K for 2 h, and subsequently annealed for 10 min at (**a**) 623 K, (**b**) 643 K, (**c**) 723 K, respectively.

To investigate the crystal structure transformation, ED patterns were collected using TEM from the alloy annealed at 643 K. Figure 5a shows a bright-field image of the sample and the ED patterns shown in Figure 5b–d corresponded to the position B, C, and D in Figure 5a, respectively. The ED pattern in Figure 5b can be assigned to the 18R-type LPSO structure model in Reference [5] The $(00018)_{18R}$ refractions, which were consistent with $(0002)_{2H}$, were divided into five refractions. In the ED patterns in Figure 5c, $(0001)_{2H}$ refraction became clearer, however, the other four refractions became unclear. Further, in Figure 5d, only $(0002)_{2H}$ and $(0001)_{2H}$ refractions remained, whereas other refractions became streaks. The c-axis of three ED patterns in Figure 5b–d is the co-axis.

Here, the structure indicated by the ED pattern of Figure 5d will be discussed. Most refractions in Figure 5d can be assigned to the 2H-Mg, however, some refractions that have to disappear due to the extinction rule, such as 0001 of 2H, can be confirmed. Further, there are strong streaks along c-axis direction. Moreover, in the bright field image in Figure 5e, many thin lines perpendicular to the c-axis are confirmed. According to these results, ABAB stacking on the c-axis are disturbed by the plain defect perpendiculer to the c-axis. Therefore, it is considered that SFs may disturb the ABAB stacking of the c-axis.

In previous studies, similar ED patterns as in Figure 5d were reported [8,15,22]. In the case of $Mg_{97}Zn_1Gd_2$, the alloy forms 14H-type LPSO with an increase in the annealing temperature [8]. The similar ED pattern and bright field image to Figure 5d,e were observed in the alloy at a lower temperature than when the 14H-type LPSO emerged. They concluded the 2H structure including a lot of SFs emerge before 14H-type LPSO formation [8]. Furthermore, in the case of $Mg_{97}Zn_1Y_2$ annealed at 573 K for 120 h, a similar ED pattern to Figure 5d was observed in the α-Mg matrix [22]. This result also explained the ED pattern caused by 2H+SFs. A recent study for $Mg_{97}Zn_1Y_2$ also reported a similar ED pattern to Figure 5d [15]. Corresponding HAADEF-STEM images indicated a lamellae structure consisting of a dark α-Mg phase and thin bright line. In the paper, the thin bright lines were expressed as "thin LPSO". Furthermore, recent atomic resolution HAADEF-STEM studied for the Mg–Zn–Gd and Mg–Zn–Y ternary alloy revealed the solute atoms enriched in SF before growing as an LPSO [14,16]. Considering thickness, the "thin LPSO" in Reference [15] would be corresponding to the solute enriched SF (SESF) reported in [16]. According to

the Figure 5 and previous results [8,15,16,22], random SF emerged before LPSO formation. Taking these reports into account, we consider the solute atoms concentrate in SF at almost the same time, which is expected by theoretical calculations [10,13,16]. This will be a formation process where the solute concentration is lower than the ideal composition of 18R-type LPSO.

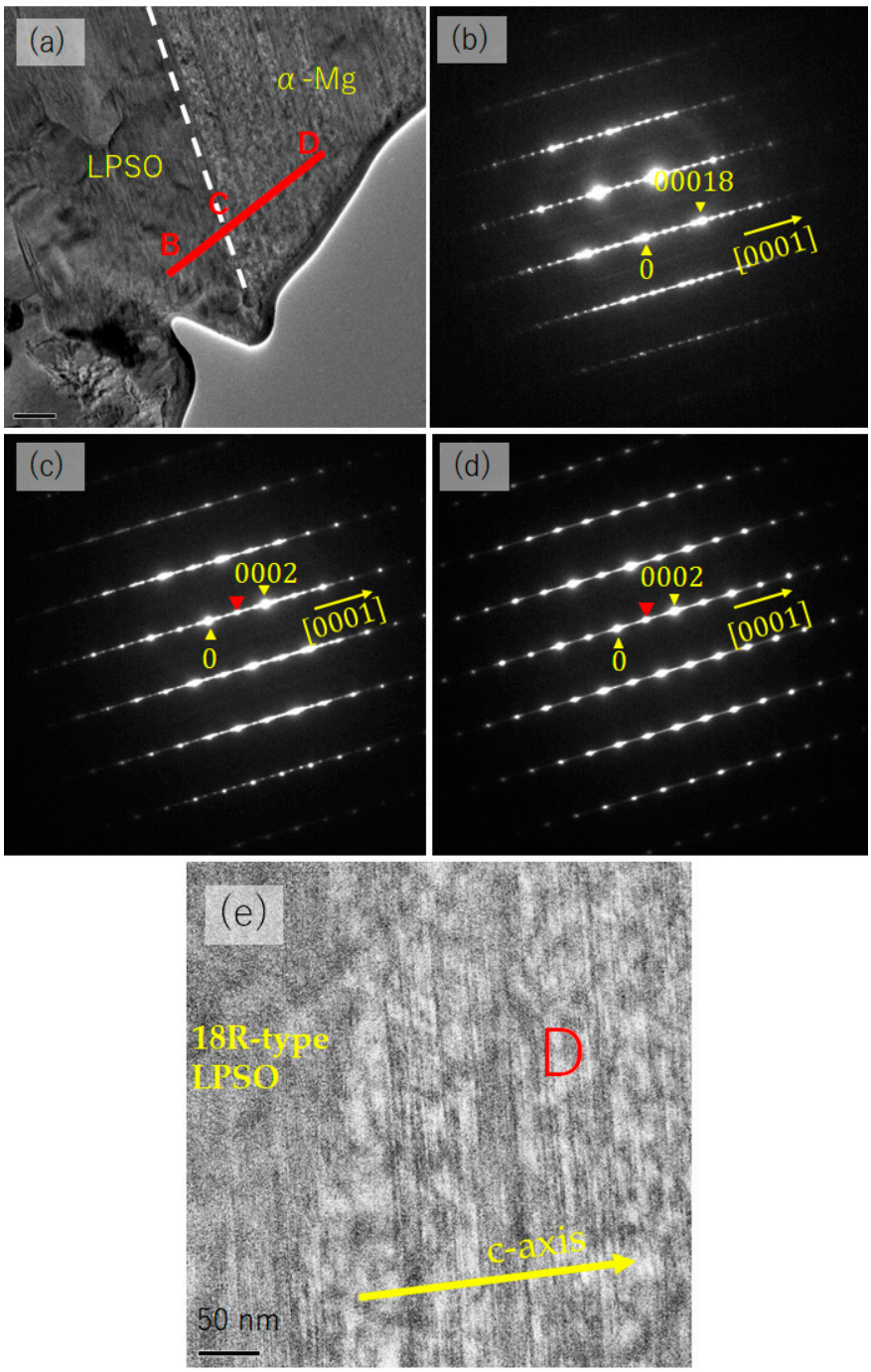

Figure 5. Bright-field image of the boundary region between α-Mg and the LPSO structures in (**a**). The electron diffraction patterns corresponding to positions B, C, and D in (**a**) are shown in (**b**–**d**), respectively. The refraction spots in (**b**) was assigned to 18R-type LPSO. The (**c**,**d**) was assigned by 2H structures, respectively. Red triangles (▼) in (**c**,**d**) is corresponding to 0001 refractions of 2H. Higher magnification bright field image around position D in (**a**) is show in (**e**).

From here, the intermediate phase, the E phase, is reported. We discovered ED patterns corresponding to the E phase [13], which is double the $D0_3$ lattice constant (Figure 6). Figure 6a,b shows ED patterns for the same parts observed by different incident beam directions. In Figure 6, spots were assigned using the $D0_3$ lattice with a lattice constant of 0.71 nm. $D0_3$ refractions divided a spot (○), i.e., the ED patterns indicated the existence of cubic structure with a lattice constant twice that of $D0_3$, which corresponded to the lattice size of the E phase. Based on these facts, the XRD peaks of E_1, E_2, E_3, ◇ and those of $D0_3$ were indexed by a E phase with a lattice constant of 1.42 nm (Table 2). The E phase is considered as fcc lattice from the extinction rule of XRD. These results indicate the E phase exists in double the number of $D0_3$ lattices as an intermediate state between $D0_3$ and LPSO.

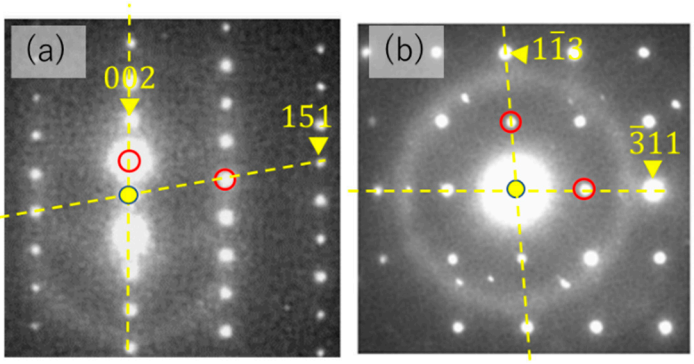

Figure 6. Electron diffraction patterns corresponding to the E phase with twice the lattice constant of $D0_3$. Incident electron beams in (**a**,**b**) are parallel to [510] and [521], respectively. The spots are assigned by the $D0_3$ structure.

Table 2. XRD peaks list corresponding to E phase with a lattice constant of 1.426 nm. The XRD pattern is the alloy annealed at 643 K in Figure 3.

Peaks	2 Theta	*d*-Value (nm)	Hkl	Difference (%)
E1	10.7	0.8258	(111)	0.1493
Labeled ◇	17.4	0.5089	(220)	0.0924
E2	20.7	0.4286	(113)	0.0290
(111) of D03	21.6	0.4109	(222)	0.0147
(200) of D03	25	0.3558	(400)	0.0130
E3	27.3	0.3263	(133)	0.0139

Next, we report on the process of the E phase collapse. A weak contrast change in the lamella pattern was observed in the alloy annealed at 643 K (Figure 7a). Lamellae parts were sectioned for TEM observation. The bright-field image and the ED pattern corresponding to the bright area indicated by an arrow are shown in Figure 7b. The ED pattern corresponded to α-Mg, where the incident beam was parallel to <0001>. The ED patterns obtained from the dark part indicated by C in Figure 7b are shown in Figure 7c. Many refractions exist, and the bright refractions can be analyzed by E phase with the incident beam direction parallel to [110]. The $[1\bar{1}1]$ and $[\bar{1}11]$ of fcc intersected at an angle of 109°. Enlarged views are given as an inset in (c). The obscure reflections indicated by yellow arrows, confirmed only among $\bar{1}11$ refractions, despite $[1\bar{1}1]$ and $[\bar{1}11]$ being equivalent directions in fcc. These refractions can be observed in a transformation process from fcc to long-period stacking, similar to a transformation from 3C to 6H in natural ZnS [23]. Figure 7d shows the ED pattern at the boundary between the fcc and α-Mg. The four spots on $[1\bar{1}1]$ fcc divided 1100 of hcp, and $[\bar{1}11]$ fcc is parallel to $[2\bar{3}10]$ direction of the α-Mg. In this case, both phases do not have shared stacking direction.

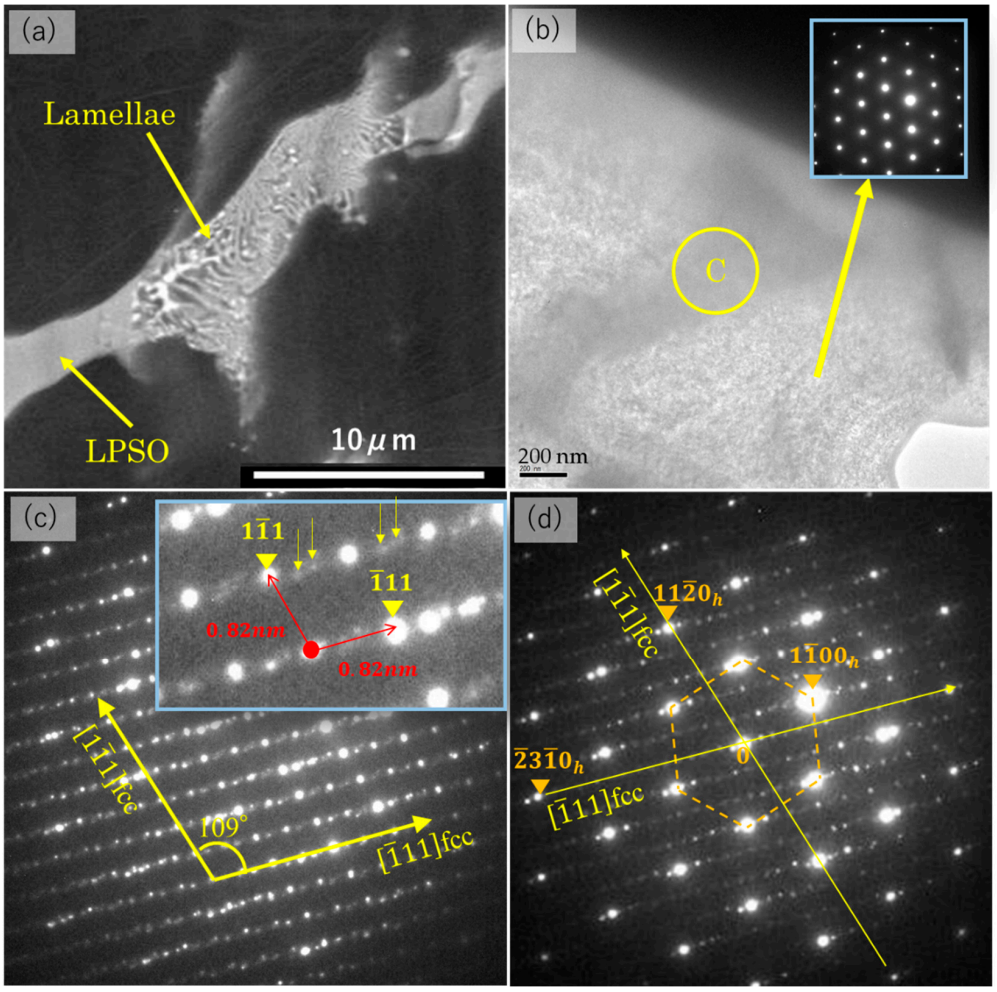

Figure 7. (**a**) Compositional image of BE mode of SEM for $Mg_{97}Zn_1Y_2$ alloy annealed at 643 K, which had been recovered after being annealed at 3 GPa and 823 K for 2 h. (**b**) Bright-field TEM image. The inset is the ED pattern of the bright phase indicated by an arrow. (**c**) The ED patterns of the locations of C in (**b**). An enlarged view of the ED pattern is shown as an inset. Refractions are assigned by the E phase, i.e., fcc with a lattice constant of 1.42 nm. (**d**) The ED patterns at the boundary between (**c**) and α-Mg. *h* means the index of hcp.

If the E phase transformed to LPSO, the microstructure and the orientation to the matrix would be different from those formed from α-Mg via SESFs. Previous research on $Mg_{97}Zn_1Gd_2$ highlighted the possibility of the existence of two kinds of LPSO formation processes [8]. One was mentioned concerning Figure 5; the LPSO precipitated into the matrix and increased the yield strength. Another is the decomposition of Mg_3Gd with the $D0_3$ structure; the LPSO has a block shape and does not increase yield strength. The latter feature is analogous to the formation of LPSO via the E phase.

4. Conclusions

1. At a pressure of 3 GPa and above 773 K, as-cast $Mg_{97}Zn_1Y_2$ alloy consisting of α-Mg matrix and 18R-type LPSO structure undergoes structural phase transformation, forming $D0_3$ superlattices in the α-Mg matrix.
2. The alloy consisting of the α-Mg matrix and $D0_3$ superlattices transformed into the α-Mg matrix and 18R-LPSO phase upon annealing at ambient pressure.
3. Considering from TEM observation results, 18R-type LPSO was continuously present with the 2H phase containing a large number of SFs. When combined with previous report [14,16], the solute atoms concentrate in SF at the almost same time, which is

expected by theoretical calculations [10,13,16]. This will be a formation process in the part where the solute concentration is lower than the ideal composition of 18R-type LPSO.

4. In the collapse process of the 18R-type LPSO structure under high-pressure and the formation process of the 18R-type LPSO structure at ambient pressure, an intermediate fcc structure with a lattice parameter of 1.42 nm (E phase), which is twice that of $D0_3$, emerged. The E phase is considered an intermediate structure between 18R-type LPSO and $D0_3$.
5. TEM observations for the E phase of the beam direction parallel to [110] confirmed obscure reflections on $[\bar{1}11]$ drections, but they were not confirmed in $[1\bar{1}1]$, though being equivalent directions in fcc. These results indicate the collapse of E phase. Further, these variations of refractions look like a transformation process from fcc to long period stacking, which is observed in natural ZnS from 3C to 6H [23].

Author Contributions: Conceptualization, M.M.; methodology, M.M.; investigation, A.Y., D.Y., N.G., M.M., T.S., M.Y., Y.K.; data curation, A.Y., N.G., D.Y., M.Y. and M.M.; writing—original draft preparation, M.M.; writing—review and editing, A.Y. and M.M.; visualization, A.Y. and M.M.; supervision, M.M. All authors have read and agreed to the published version of the manuscript.

Funding: This research was supported by a MEXT Grant-in-Aid for Scientific Research (No. 19K04987), The Light Metal Educational Foundation (2019–2020), and JKA (2018M128).

Data Availability Statement: All data used the article was kept in Ehime University by some authors (A.Y., D.Y., and M.M.).

Acknowledgments: Authors acknowledge to Hiroaki Ohfuji, Tohoku University and Masahiro Fukuda, Ehime University for technical help of TEM observations.

Conflicts of Interest: The authors declare no conflict of interest.

References

1. Kawamura, Y.; Hayashi, K.; Inoue, A.; Masumoto, T. Rapidly solidified powder Metallurgy $Mg_{97}Zn_1Y_2$ alloys with excellent tensile yield strength above 600 MPa. *Mater. Trans.* **2001**, *42*, 1172–1176. [CrossRef]
2. Shao, X.H.; Jin, Q.Q.; Zhou, Y.T.; Yang, H.J.; Zheng, S.J.; Zhang, B.; Chen, Q.; Ma, X.L. Basal shearing of twinned stacking faults and its effect on mechanical properties in an Mg–Zn–Y alloy with LPSO phase. *Mater. Sci. Eng. A* **2020**, *779*, 139109. [CrossRef]
3. Hagihara, K.; Ueyama, R.; Yamasaki, M.; Kawamura, Y.; Nakano, T. Surprising Increase in Yield Stress of Mg Single Crystal Using Long-Period Stacking Ordered Nanoplates. *Acta Mater.* **2021**, *209*, 116797. [CrossRef]
4. Liu, C.; Zhu, Y.; Luo, Q.; Liu, B.; Gu, Q.; Li, Q. A 12R Long-Period Stacking-Ordered Structure in a Mg-Ni-Y Alloy. *J. Mater. Sci. Technol.* **2018**, *34*, 2235–2239. [CrossRef]
5. Egusa, D.; Abe, E. The Structure of Long Period stacking/Order Mg–Zn–RE Phases With Extended Non-Stoichiometry Ranges. *Acta Mater.* **2012**, *60*, 166–178. [CrossRef]
6. Yamasaki, M.; Matsushita, M.; Hagihara, K.; Izuno, H.; Abe, E.; Kawamura, Y. Highly Ordered 10H-Type Long-Period Stacking Order Phase in a Mg–Zn–Y Ternary Alloy. *Scr. Mater.* **2014**, *78-79*, 13–16. [CrossRef]
7. Saal, J.; Wolverton, C. Thermodynamic Stability of Mg-Based Ternary Long-Period Stacking Ordered Structures. *Acta Mater.* **2014**, *68*, 325–338. [CrossRef]
8. Yamasaki, M.; Sasaki, M.; Nishijima, M.; Hiraga, K.; Kawamura, Y. Formation of 14H Long Period Stacking Ordered Structure and Profuse Stacking Faults in Mg–Zn–Gd Alloys During Isothermal Aging at High Temperature. *Acta Mater.* **2007**, *55*, 6798–6805. [CrossRef]
9. Iikubo, S.; Matsuda, K.; Ohtani, H. Phase Stability of Long-Period Stacking Structures in Mg-Y-Zn: A First-Principles Study. *Phys. Rev. B* **2012**, *86*, 054105. [CrossRef]
10. Iikubo, S.; Hamamoto, S.; Ohtani, H. Thermodynamic Analysis of the Mg–RE–Zn (RE = Y, La) Ternary Hcp Phase Using the Cluster Variation Method. *Mater. Trans.* **2013**, *54*, 636–640. [CrossRef]
11. Okuda, H.; Yamasaki, M.; Kawamura, Y.; Tabuchi, M.; Kimizuka, H. Nanoclusters First: A Hierarchical Phase Transformation in a Novel Mg Alloy. *Sci. Rep.* **2015**, *5*, 14186. [CrossRef] [PubMed]
12. Liu, H.; Bai, J.; Yan, K.; Yan, J.; Ma, A.; Jiang, J. Comparative Studies on Evolution Behaviors of 14H LPSO Precipitates in As-Cast and As-Extruded Mg–Y–Zn Alloys During Annealing at 773K. *Mater. Des.* **2016**, *93*, 9–18. [CrossRef]
13. Matsushita, M.; Nagata, T.; Bednarcik, J.; Nishiyama, N.; Kawano, S.; Iikubo, S.; Kubota, Y.; Morishita, R.; Irifune, T.; Yamasaki, M.; et al. Key Factor for the Transformation from Hcp to 18R-Type Long-Period Stacking Ordered Structure in Mg Alloys. *Mater. Trans.* **2019**, *60*, 237–245. [CrossRef]

14. Egusa, D.; Kawaguchi, K.; Abe, E. Direct Observations of Precursor Short-Range Order Clusters of Solute Atoms in a LPSO-Forming Mg-Zn-Gd Ternary Alloy. *Front. Mater.* **2019**, *6*, 266. [CrossRef]
15. Jin, Q.Q.; Shao, X.H.; Yang, L.X.; Zhou, Y.T.; Zhang, B.; Zheng, S.J.; Ma, X.L. Stacking faults and growth twins in long-period stacking ordered structures in a near-equilibrium $Mg_{97}Zn_1Y_2$ alloy. *Mater. Charact.* **2020**, *165*, 11039. [CrossRef]
16. Egami, M.; Ohnuma, I.; Enoki, M.; Ohtani, H.; Abe, E. Thermodynamic Origin of Solute-Enriched Stacking-Fault in Dilute Mg-Zn-Y Alloys. *Mater. Des.* **2020**, *188*, 108452. [CrossRef]
17. Itakura, M.; Yamaguchi, M.; Egusa, D.; Abe, E. Density Functional Theory Study of Solute Cluster Growth Processes in Mg-Y-Zn LPSO Alloys. *Acta Mater.* **2021**, *203*, 116491. [CrossRef]
18. Matsushita, M.; Bednarcik, J.; Sakata, Y.; Akamatsu, S.; Nishiyama, N.; Michalikova, J.; Yamasaki, M.; Kawamura, Y. Synchronized collapse and formation of long-period stacking and chemical orders in $Mg_{85}Zn_6Y_9$. *Phys. B* **2015**, *461*, 147–153. [CrossRef]
19. Matsushita, M.; Sakata, Y.; Senzaki, T.; Yamasaki, M.; Yamada, I.; Saitoh, H.; Shinmei, T.; Irifune, T.; Nishiyama, N.; Kawamura, Y. Phase relations among $D0_3$, α-Mg, and Long-period stacking orders in $Mg_{85}Zn_6Y_9$ alloy under 3 GPa. *Mater. Trans.* **2015**, *56*, 910–913. [CrossRef]
20. Matsushita, M.; Yamamoto, S.; Nishiyama, N.; Sakata, Y.; Yamasaki, M.; Bednarcik, J.; Irifune, T.; Kawamura, Y. $D0_3$ + hcp mixed phase with nanostructures in $Mg_{85}Zn_6Y_9$ alloy obtained by high-pressure and high-temperature treatments. *Mater. Lett.* **2015**, *155*, 11–14. [CrossRef]
21. Jiang, W.; Zou, C.; Huang, H.-T.; Ran, Z.; Wei, Z. Crystal Structure and Mechanical Properties of a New Ternary Phase in Mg-Zn-Y Alloy Solidified under High Pressure. *J. Alloy. Compd.* **2017**, *717*, 214–218. [CrossRef]
22. Ono, A.; Abe, E.; Itoi, T.; Hirohashi, M.; Yamasaki, M.; Kawamura, Y. Microstructure Evolutions of Rapidly-Solidified and Conventionally-Cast $Mg_{97}Zn_1Y_2$ Alloys. *Mater. Trans.* **2008**, *429*, 990–994. [CrossRef]
23. Wu, Z.; Sun, X.; Xu, H.; Konishi, H.; Wang, Y.; Lu, Y.; Gao, K.; Wang, C.; Zhou, H. Microstructural characterization and in-situ sulfur isotopic analysis of silver bearing sphalerite from the Edmond hydrothermal field, Central Indian Ridge. *Ore Geol. Rev.* **2018**, *92*, 318–347. [CrossRef]